

QUANTIFYING HUMAN IMPACT ON THE 2018 SUMMER LONGEST HEAT WAVE IN SOUTH KOREA

SEUNG-KI MIN, YEON-HEE KIM, SANG-MIN LEE, SARAH SPARROW,
SIHAN LI, FRASER C. LOTT, AND PETER A. STOTT

High-resolution large-ensemble simulations indicate that human activities have at least quadrupled the probability of occurrence of the extremely long-lasting heat waves over South Korea as observed in 2018 summer.

During summer 2018, South Korea experienced the strongest and longest heat wave since 1973 (the beginning of the observations from 45 stations). The July–August (JA) mean daily maximum temperature (T_{\max}) was on average 2.6°C warmer than 1987–2010 climatology over South Korea, setting its second highest record after 1994 (Figs. 1a,c). A simple analysis based on a long-term CRU TS data suggests that the return time of 2018 T_{\max} is about 26 years, much shorter than about 386 years in 1912 (Fig. ES1), although a large uncertainty related to data homogeneity and urbanization effect should be noted (Park et al. 2017). Unusually hot weather led to record-breaking temperatures over many stations with temperature $> 40^{\circ}\text{C}$ at some stations for the first time. More importantly, the 2018 heat wave had the longest duration on record with 31.5 hot days (total number of days with daily maximum temperature $> 33^{\circ}\text{C}$) surpassing the previous record of 29.7 days in 1994, and exerted considerable impacts on society and the economy (reported in the *Korea*

Herald^{1,2}), including 48 heat-related deaths (KCDC 2018). The heat wave also induced crop destruction in North Korea.³ When using a heat wave duration index (HWDx) defined as maximum consecutive hot days during summer, the 2018 record is extremely high at 18.1 days (Figs. 1b,d). There is a strong correlation between JA mean T_{\max} and HWDx ($r = 0.74$; Figs. 1c,d), indicating a close relation between mean warming and heat wave duration. This long-lasting heat wave is characterized by a persistent anomalous high pressure system in the upper troposphere over Korea (Fig. 1f), which seems to be partly induced by the strong tropical convection over northwestern India and the South China Sea (Fig. 1e), through the well-known teleconnection mechanism (Fig. 1g; Lee and Lee 2016; Kim et al. 2019; Yeo et al. 2019).

This study aims at quantifying human contribution to the 2018 summer longest duration of heat wave in South Korea. The long duration of heat wave is known to be critically important for health (e.g., Anderson and Bell 2011; D'Ippoliti et al. 2010). To address this question for small spatial scale, we utilize high-resolution large-ensemble regional climate model (RCM) (weather@home East Asia; 50 km) and global climate model (GCM) (HadGEM3-A-N216; 60 km at midlatitudes) simulations, each performed with and without anthropogenic forcings (Table ES1). Comparing two models will help assess the confidence of the resulting attribution statement even though both models are from the Hadley model fam-

AFFILIATIONS: MIN, KIM, AND LEE—Division of Environmental Science and Engineering, Pohang University of Science and Technology, Pohang, Gyeongbuk, South Korea; SPARROW AND LI—Oxford e-Research Centre, Department of Engineering, University of Oxford, Oxford, United Kingdom; LOTT AND STOTT—Met Office, Exeter, United Kingdom

CORRESPONDING AUTHOR: Seung-Ki Min, skmin@postech.ac.kr

DOI:10.1175/BAMS-D-19-0151.1

A supplement to this article is available online (10.1175/BAMS-D-19-0151.2)

© 2019 American Meteorological Society
For information regarding reuse of this content and general copyright information, consult the [AMS Copyright Policy](#).

¹ http://www.koreaherald.com/view.php?ud=20180808000476&ACE_SEARCH=1

² http://www.koreaherald.com/view.php?ud=20180821000128&ACE_SEARCH=1

³ <https://www.theguardian.com/world/2018/aug/09/south-korean-heatwave-causes-record-deaths>

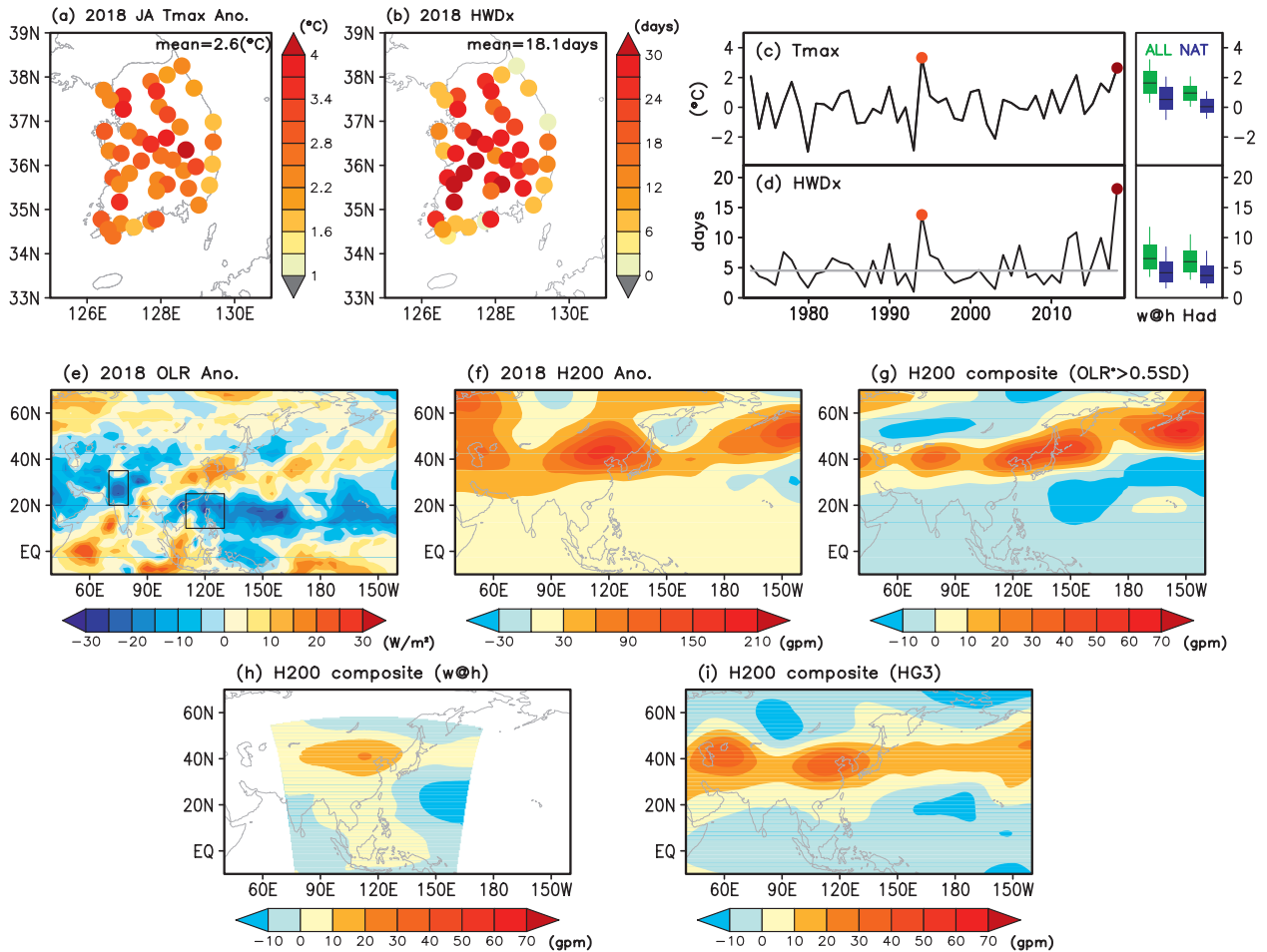


FIG. 1. Distribution of (a) 2018 JA mean daily maximum temperature (T_{\max}) anomalies and (b) 2018 JA maximum heat wave duration (HWDx), defined as the maximum consecutive hot days ($T_{\max} \geq 33^{\circ}\text{C}$) over South Korea. Also shown are observed time series of South Korean mean (c) T_{\max} anomalies and (d) HWDx over 1973–2018, and simulated ranges of 2018 T_{\max} anomalies and HWDx from w@h and HadGEM3-A-N216 experiments (box-and-whisker plots); and anomaly distribution of (e) 2018 JA mean OLR (NOAA interpolated data) and (f) 200-hPa geopotential height (NCEP1 reanalysis). Two boxes in (e) indicate the two convection zones of the northwestern India ($70^{\circ}\text{--}80^{\circ}\text{E}$, $20^{\circ}\text{--}35^{\circ}\text{N}$) and South China Sea ($110^{\circ}\text{--}130^{\circ}\text{E}$, $10^{\circ}\text{--}25^{\circ}\text{N}$), selected based on previous studies (Kim et al. 2019; Lee and Lee 2016). Finally, anomaly composites are shown of 200-hPa geopotential height for strong convection years during 1987–2010 (OLR stronger than 0.5 standard deviation) over both convection zones from (g) observations (NCEP1 reanalysis), (h) w@h, and (i) HadGEM3-A-N216 simulations. All anomalies are with respect to 1987–2010 mean.

ily. Using the risk ratio, we compare the probabilities of occurrence of the extremely long duration of heat wave between the real and counterfactual (without human influences) worlds. Further, the influences of tropical convections on the longer-lasting heat wave is examined. In this regard, RCM and GCM are found to reasonably capture the observed teleconnection pattern (cf. Figs. 1h and 1i with Fig. 1g, pattern correlation > 0.6).

DATA AND METHODS. Daily maximum temperatures (T_{\max}) from 45 South Korean weather

stations are used as observations for 1973–2018. To match the spatial scale between point observations and gridded model outputs, we interpolate daily station observations onto the HadGEM3-A-N216 grid boxes of 0.86° (longitude) \times 0.56° (latitude) by taking simple averages of station values within each grid box, assuming a high spatial correlation in daily temperature extremes (Donat et al. 2013). The observed HWDx is calculated using the gridded T_{\max} data to obtain South Korean area averaged HWDx. To consider model biases in climatology and variability in T_{\max} , we apply a different T_{\max} threshold for each

model (33.21°C for weather@home and 30.51°C for HadGEM3-A-N216), which corresponds to the same quantile as in the observed threshold (33°C). Using this method, models are found to have similar HWDx means as the observed around 4 days. The analysis domain for South Korea is 34°–38°N and 125°–130°E (land only).

Large-ensemble RCM data from weather@home (abbreviated herein as w@h) East Asia are used in which the HadRM3P RCM is simulated at a 50-km resolution over the East Asia region (domain extent shown in Fig. 1h) driven by the HadAM3P atmospheric GCM (Massey et al. 2015; Guillod et al. 2017). The real world simulations (ALL; 2,300 members) for 2018 were carried out by prescribing the observed sea surface temperature (SST) and sea ice coverage and also by implementing the observed greenhouse gas and aerosol forcings. The counterfactual world simulations (NAT; 3,700 members) for 2018 were performed by using adjusted observed SST and sea ice conditions with anthropogenic changes removed and setting other external forcings as preindustrial levels (see Table ES1 in the online supplemental material; Schaller et al. 2016). HadGEM3-A provides large-ensemble (525 members for ALL and NAT each) GCM data, which have a high resolution of $0.83^\circ \times 0.56^\circ$ (referred to as HadGEM3-A-N216; Ciavarella et al. 2018). The boundary conditions and external forcings for ALL and NAT simulations are very similar to the w@h experiment (Table ES1). One difference is that HadGEM3-A-N216 uses single estimate of the anthropogenic SST changes (delta-SST) while w@h uses 13 different estimates (Table ES2), and its influence on the attribution results is examined. We also use baseline simulations from RCM and GCM for 1987–2010 (data period of w@h runs), which provides a reference climatology for both ALL and NAT runs (Sparrow et al. 2018). Observed anomalies are also based on the 1987–2010 means. When evaluating models using the baseline runs, RCM can capture the observed interannual variabilities for both T_{\max} and HWDx but GCM tends to underestimate the T_{\max} variability. The latter seems to be associated with the lower probability of occurrence of heat waves in the GCM, and consequently our results should be interpreted with caution (see below).

The risk ratio (RR) is analyzed between ALL and NAT simulations to assess the human impact on the probability of occurrence of extreme events, which is calculated as the ratio of the probability of exceeding observed events in ALL (P_{ALL}) and NAT simulations (P_{NAT}), i.e., $\text{RR} = P_{\text{ALL}}/P_{\text{NAT}}$ (e.g., Easterling et al. 2016). RR is also calculated using 1994 observations to assess

robustness. We use the “likelihood ratio method” (Paciorek et al. 2018) to estimate the 5%–95% confidence intervals of RR, which can provide a confidence interval (at least a lower bound) even when the estimate of the RR is infinity.

RESULTS. Figure 2 shows the return period distributions of the JA mean T_{\max} anomalies and HWDx for ALL and NAT simulations from w@h and HadGEM3-A-N216. Return periods are significantly shortened for T_{\max} anomalies with human influences for both models (Figs. 2a,b). The probability of T_{\max} anomalies higher than the observed 2018 value is 19.8% in ALL (P_{ALL}) and it is reduced to 4.2% in NAT simulations (P_{NAT}) for w@h (Fig. ES2a). This makes RR as large as 4.7 (5%–95% range of 4.1–5.5), indicating that anthropogenic influences increase the risk of extremely warm summer by 4 to 5 times, well consistent with previous studies based on different models (Min et al. 2014; Kim et al. 2018). The large P_{ALL} indicates a possible influence of the observed 2018 SST condition in w@h model, which may occur in this type of single-year atmosphere-only experiment (Risser et al. 2017). A simple comparison with the 2017 experiment results suggests that the observed 2018 SST condition may contribute to a larger warming over northern East Asia including the Korea peninsula through intensified tropical convections (Fig. ES3). However, RR is unlikely to be affected much [$\text{RR} = 5.15$ (3.9–6.9) based on 2017 runs] because of similar SST impact on NAT results (Fig. ES3). HadGEM3-A-N216 has longer return periods due to lower values of P_{ALL} and P_{NAT} for T_{\max} as 3.6% and 0.19%, respectively (Fig. ES2b). This gives a larger RR of 19.0 (4.9–184), which might be in part due to the smaller sample size (cf. Sparrow et al. 2018). When using a stronger threshold (1994 T_{\max} anomalies), results remain similar with $\text{RR} = 6.5$ (5.1–8.4) for w@h and $P_{\text{NAT}} = 0\%$ for HadGEM3-A-N216 (Table ES1).

HWDx results display shortened return periods of the long-lasting heat waves under anthropogenic influences (Figs. 2c,d). The return periods are generally longer than T_{\max} for both models. P_{ALL} and P_{NAT} are very low as 1.0% and 0.11% from w@h, respectively (Fig. ES2c). The corresponding RR is 9.7 (4.3–26.1), indicating that the risk of 2018-like extremely long-lasting heat wave has increased by about 10 times due to human impacts. In HadGEM3-A-N216, extreme heat wave events longer than the observed 2018 values are extremely rare even with human-induced warming ($P_{\text{ALL}} = 0.76\%$) and no events are present without human influences ($P_{\text{NAT}} = 0\%$; Fig. ES2d). Although the probability might be this low due to

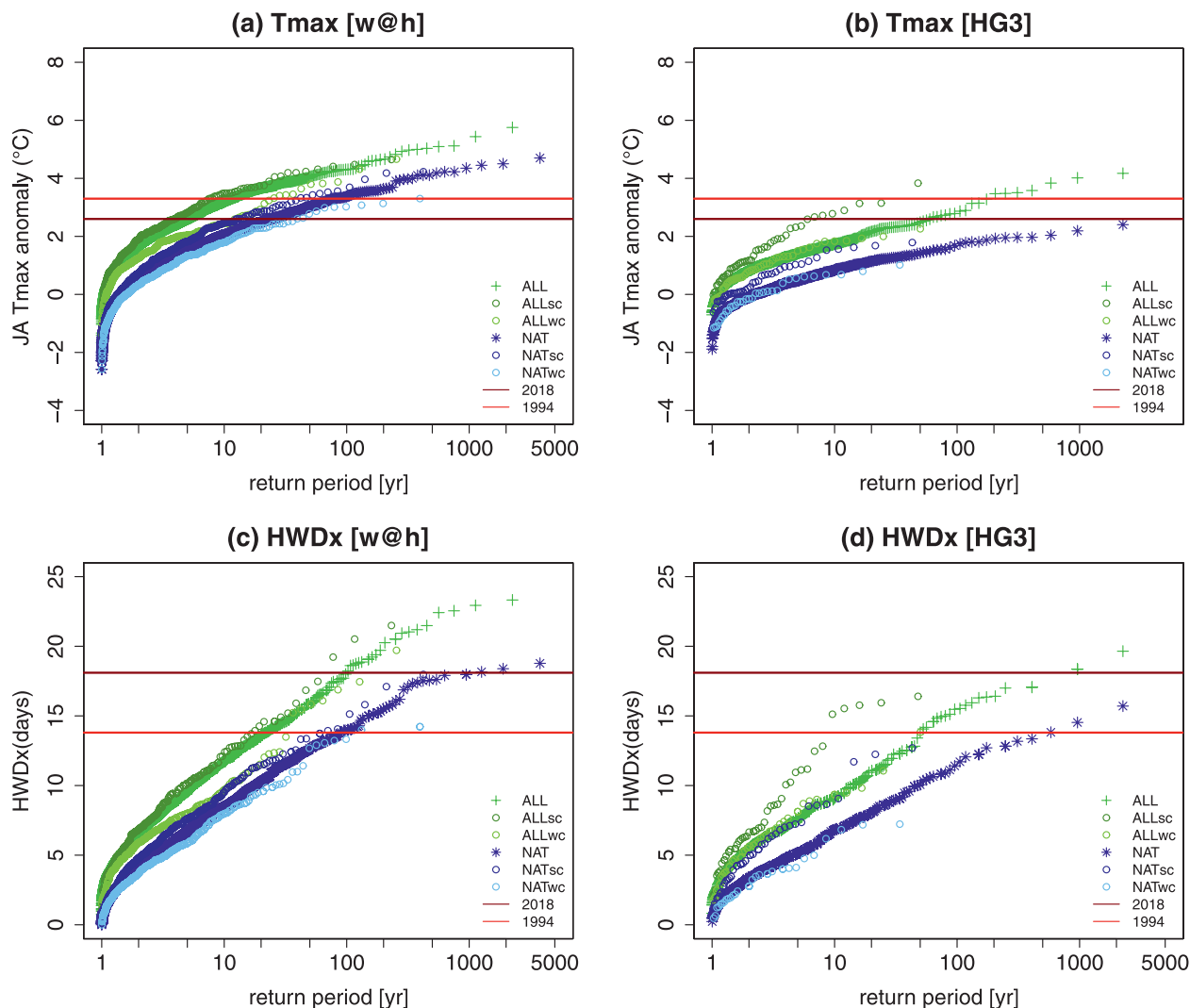


FIG. 2. Return periods of (a),(b) the JA mean T_{\max} anomalies and (c),(d) HWDx for ALL (green) and NAT (blue) simulations from w@h and HadGEM3-A-N216 (HG3). Kernel density distributions in Fig. ES2 are used to estimate return periods. The purple and red horizontal lines indicate the observed 2018 and 1994 values, respectively. Minor ticks on the x axis indicate 2, 5, 20, 50, 200, 500, etc. Results from subsampled ensemble members are displayed with stronger (OLR below the 30th percentile; ALLsc and NATsc) and weaker convection (OLR above the 70th percentile; ALLwc and NATwc) over two convection zones (see Fig. 1e). For HadGEM3-A-N216, precipitation is used instead of OLR. Refer to Table ES1 for corresponding RR values.

the small sample size and the smaller variability of HadGEM3-A-N216 as mentioned above, the consistent shift of the probability distribution indicates the increased risk of extreme events due to anthropogenic warming. When using the 1994 observed value (13.8 days, second highest record) as another observed threshold, results support this conclusion, providing a large RR of 5.8 (2.6–15.6) with $P_{\text{ALL}} = 4.4\%$ and $P_{\text{NAT}} = 0.8\%$ (Table ES1). For w@h, the RR remains large as 4.1 (3.9–5.5).

To examine the influence of boundary SST conditions estimated for NAT (see above), we have divided

the w@h ensembles into 13 groups based on the delta-SSTs provided by GCMs (see Table ES2) and repeated our RR analysis. Results show a large spread in RRs across the delta-SST estimates (Fig. ES4), which is found to be significantly related to the different aerosol sensitivity of GCMs that provide the delta-SSTs, reaffirming previous studies (Kim et al. 2018; Min et al. 2019). In spite of the large spread, RRs remain larger than unity in all cases, which supports that the probability of occurrence of 2018-like summer heat wave intensity and maximum duration has increased due to the human activities.

To explore the extent to which the stronger tropical convection has contributed to the 2018 extreme heat wave, we have compared the T_{\max} and HWDx distributions constructed from samples with stronger tropical convection with those with weaker tropical convection. The samples with stronger (weaker) convection were selected when OLR anomalies over two convection zones (black boxes in Fig. 1e) are below the 30th percentile (above the 70th percentile). For HadGEM3-A-N216, precipitation was used to construct the distributions because OLR data are not available. Results show that when the tropical convection is stronger, the return times of extreme events decrease for both T_{\max} and HWDx, and vice versa (Fig. 2). Accordingly, P_{ALL} increases from 19.8% to 25.9% and P_{NAT} increases from 4.2% to 7.8% for T_{\max} from w@h. For HWDx, P_{ALL} increases from 1.0% to 1.7% from w@h and 0.76% to 2.1% from HadGEM3-A-N216 (Fig. ES2). However, the resulting RRs remain overall similar, larger than 3 (Table ES1), indicating consistent human influences on the increased intensity and the extended duration of heat wave, irrespective of the influence of tropical convection. Nevertheless, disproportionate responses in RRs to convection strengths between ALL and NAT imply that the SST warming pattern prescribed can be important (Risser et al. 2017).

CONCLUDING REMARKS. High-resolution large-ensemble simulations from an atmospheric RCM (w@h) and an atmospheric GCM (HadGEM3-A-N216) consistently show increases in the likelihood of a 2018-like extreme heat wave intensity and maximum duration by at least 4 times, when including anthropogenic forcing (mainly due to greenhouse gas increases). Further, comparisons of sub-sampled model simulations suggest that strong tropical convection activity over two regions (northwestern India and South China Sea) seems to have contributed to the increased probability of the heat wave intensity and duration by up to a factor of 2. However, human influences on heat waves, as quantified by RR values, remain overall unaffected by the strength of tropical convection, suggesting that the local thermodynamic factor would be more important than the non-local factors including large-scale teleconnection changes.

ACKNOWLEDGMENTS. This work was supported by the Korea Meteorological Administration Research and Development Program under Grants KMI2018-01214 and 1365003000 and by a National Research Foundation of Korea (NRF) grant funded by the South Korean government (MSIT) (NRF-2018R1A5A1024958). We thank the

Met Office Hadley Centre PRECIS team for their technical and scientific support for the development and application of weather@home. We also thank all of the volunteers who have donated their computing time to climateprediction.net and weather@home. Fraser C. Lott and Peter A. Stott were supported by the U.K.–China Research and Innovation Partnership Fund through the Met Office Climate Science for Service Partnership (CSSP) China as part of the Newton Fund.

REFERENCES

- Anderson, G. B., and M. L. Bell, 2011: Heat waves in the United States: Mortality risk during heat waves and effect modification by heat wave characteristics in 43 U.S. communities. *Environ. Health Perspect.*, **119**, 210–218, <https://doi.org/10.1289/ehp.1002313>.
- Ciavarella, A., and Coauthors, 2018: Upgrade of the HadGEM3-A based attribution system to high resolution and a new validation framework for probabilistic event attribution. *Wea. Climate Extremes*, **20**, 9–32, <https://doi.org/10.1016/j.wace.2018.03.003>.
- D'Ippoliti, D., and Coauthors, 2010: The impact of heat waves on mortality in 9 European cities: results from the EuroHEAT project. *Environ. Health*, **9**, 37, <https://doi.org/10.1186/1476-069X-9-37>.
- Donat, M. G., and Coauthors, 2013: Updated analyses of temperature and precipitation extreme indices since the beginning of the twentieth century: The HadEX2 dataset. *J. Geophys. Res.*, **118**, 2098–2118, <https://doi.org/10.1002/JGRD.50150>.
- Easterling, D. R., K. E. Kunkel, M. F. Wehner, and L. Sun, 2016: Detection and attribution of climate extremes in the observed record. *Wea. Climate Extremes*, **11**, 17–27, <https://doi.org/10.1016/j.wace.2016.01.001>.
- Guilod, B. P., and Coauthors, 2017: weather@home2: Validation of an improved global-regional climate modeling system. *Geosci. Model Dev.*, **10**, 1849–1872, <https://doi.org/10.5194/gmd-10-1849-2017>.
- KCDC, 2018: Annual report on the notified patients with heat-related illness in Korea (in Korean). Korea Centers for Disease Control and Prevention, 56 pp.
- Kim, M.-K., J.-S. Oh, C.-K. Park, S.-K. Min, K.-O. Boo, and J.-H. Kim, 2019: Possible impact of the diabatic heating over the Indian subcontinent on heat waves in South Korea. *Int. J. Climatol.*, **39**, 1166–1180, <https://doi.org/10.1002/joc.5869>.
- Kim, Y.-H., S.-K. Min, D. A. Stone, H. Shiogama, and P. Wolski, 2018: Multi-model event attribution of the summer 2013 heat wave in Korea. *Wea. Climate Extremes*, **20**, 33–44, <https://doi.org/10.1016/j.wace.2018.03.004>.

- Lee, W.-S., and M.-I. Lee, 2016: Interannual variability of heat waves in South Korea and their connection with large-scale atmospheric circulation patterns. *Int. J. Climatol.*, **36**, 4815–4830, <https://doi.org/10.1002/joc.4671>.
- Massey, N., and Coauthors, 2015: weather@home—Development and validation of a very large ensemble modelling system for probabilistic event attribution. *Quart. J. Roy. Meteor. Soc.*, **141**, 1528–1545, <https://doi.org/10.1002/qj.2455>.
- Min, S.-K., Y.-H. Kim, M.-K. Kim, and C. Park, 2014: Assessing human contribution to the summer 2013 Korean heat wave [In “Explaining Extreme Events of 2013 from a Climate Perspective”]. *Bull. Amer. Meteor. Soc.*, **95**, S48–S51, <https://journals.ametsoc.org/doi/pdf/10.1175/1520-0477-95.9.S1.1>.
- , —, I.-H. Park, D. Lee, S. Sparrow, D. Wallom, and D. Stone, 2019: Anthropogenic contribution to the 2017 earliest summer onset in South Korea. *Bull. Amer. Meteor. Soc.*, **100** (1), S73–S77, <https://doi.org/10.1175/BAMS-D-18-0096.1>.
- Paciorek, C. J., D. A. Stone, and M. F. Wehner, 2018: Quantifying statistical uncertainty in the attribution of human influence on severe weather. *Wea. Climate Extremes*, **20**, 69–80, <https://doi.org/10.1016/j.wace.2018.01.002>.
- Park, B.-J., Y.-H. Kim, S.-K. Min, M.-K. Kim, Y. Choi, K.-O. Boo, and S. Shim, 2017: Long-term warming trends in Korea and contribution of urbanization: An updated assessment. *J. Geophys. Res.*, **122**, 10 637–10 654, <https://doi.org/10.1002/2017JD027167>.
- Risser, M. D., D. A. Stone, C. J. Paciorek, M. F. Wehner, and O. Angélil, 2017: Quantifying the effect of interannual ocean variability on the attribution of extreme climate events to human influence. *Climate Dyn.*, **49**, 3051–3073, <https://doi.org/10.1007/s00382-016-3492-x>.
- Schaller, N., and Coauthors, 2016: Human influence on climate in the 2014 southern England winter floods and their impacts. *Nat. Climate Change*, **6**, 627–634, <https://doi.org/10.1038/nclimate2927>.
- Sparrow, S., and Coauthors, 2018: Attributing human influence on the July 2017 Chinese heatwave: The influence of sea-surface temperatures. *Environ. Res. Lett.*, **13**, 114004, <https://doi.org/10.1088/1748-9326/aac356>.
- Yeo, S.-R., S.-W. Yeh, and W.-S. Lee, 2019: Two types of heat wave in Korea associated with atmospheric circulation pattern. *J. Geophys. Res.*, **124**, 7498–7511, <https://doi.org/10.1029/2018JD030170>.